Dynamics of a pre-lens tear film after a blink: Model, evolution, and rupture

R. Usha, Anjalaiah, and Y. V. S. S. Sanyasiraju

Citation: Physics of Fluids (1994-present) **25**, 112111 (2013); doi: 10.1063/1.4831795
View online: http://dx.doi.org/10.1063/1.4831795
View Table of Contents: http://scitation.aip.org/content/aip/journal/pof2/25/11?ver=pdfcov
Published by the AIP Publishing

PHYSICS OF FLUIDS **25**, 112111 (2013)

Dynamics of a pre-lens tear film after a blink: Model, evolution, and rupture

R. Usha,[a] Anjalaiah,[b] and Y. V. S. S. Sanyasiraju[c]
Department of Mathematics, Indian Institute of Technology Madras, Chennai 600 036, India

(Received 16 April 2013; accepted 27 October 2013; published online 27 November 2013)

A mathematical model is developed to investigate the dynamics and rupture of a pre-lens tear film on a contact lens. The contact lens is modeled as a saturated porous medium of constant, finite thickness and is described by the Darcy-Brinkman equations with stress-jump condition at the interface. The model incorporates the influence of capillarity, gravitational drainage, contact lens properties such as the permeability, the porosity, and the thickness of the contact lens on the evolution and rupture of a pre-lens tear film, when the eyelid has opened after a blink. Two models are derived for the evolution of a pre-lens tear film thickness using lubrication theory and are solved numerically; the first uses shear-free surface condition and the second, the tangentially immobile free surface condition. The results reveal that life span of a pre-lens tear film is longer on a thinner contact lens for all values of permeability and porosity parameter considered. An increase in permeability of contact lens, porosity or stress-jump parameter increases the rate of thinning of the film and advances the rupture time. The viscous-viscous interaction between the porous contact lens and the pre-lens tear film increases the resistance offered by the frictional forces to the rate of thinning of pre-lens tear film. This slows down the thinning process and hence delays the rupture of the film as compared to that predicted by the models of Nong and Anderson [SIAM. J. Appl. Math. **70**, 2771–2795 (2010)] derived in the framework of Darcy model. [http://dx.doi.org/10.1063/1.4831795]

I. INTRODUCTION

The surface of the eye is protected by a tear film that provides an optically smooth interface, removes foreign bodies and lubricates the gap between the eyelids and the cornea of the eye.[1] The human tear film is most often described as comprising three distinct layers; an outermost bi-component oily lipid layer[2–5](typical thickness 100 nm), an innermost mucus layer (typical thickness 0.5–1.0 μm), and an intermediate aqueous layer[6–13] (typical thickness 4–10 μm). The sacks under the lower and the upper lids are filled with the aqueous component of tear film and it is supplied by the main accessory lacrimal glands.[7,14] The lipid layer is composed mainly of Meibomian lipid secreted from the Meibomian glands.[15] The lipid layer reduces evaporation of the aqueous fluid in the tear film and decreases the surface tension at the tear film/air interface. It stabilizes the tear film against rupture due to its higher viscosity and lower surface tension. The mucus layer is secreted from cells that are located in the conjunctival epithelium and helps to promote wetting of the cornea by transporting away non wettable debris. Recent views claim that mucus layer blends with the aqueous layer without any interfacial tension between the two.[15–19] This suggests that the three layer theory must be replaced by one in which the mucins secreted from the goblet cells are distributed throughout the mucoaqueous layer which forms the bulk of the tear film and epithelial mucins form a complex barrier at the corneal surface.

[a]Author to whom correspondence should be addressed. Electronic mail: ushar@iitm.ac.in
[b]Email: anjimaths20@gmail.com
[c]Email: sryedida@iitm.ac.in

The tear film on the cornea referred to as a pre-corneal tear film, the pre-lens, and the post-lens tear film that arise in the presence of a contact lens and pre-conjunctival tear film are the three main classifications of the tear film. Immediately after a blink, tear film begins to evolve due to the effects of gravity and evaporation. These effects cause holes in the tear film resulting in a condition known as dry-eye syndrome.

Motivated by the need to contribute to medical knowledge for diseased conditions such as dry-eye syndrome, there have been several theoretical reports describing the dynamics of pre-corneal tear film.[10–13,20–31] The investigations by Wong *et al.*,[21] Braun and Fitt,[13] and Jones *et al.*[32] have computed the thickness of the tear film after blinking and their approach is based on modeling the tear film as an aqueous layer influenced by gravity, viscosity, surface tension, and evaporation effects. These models show that thinning of the tear film occurs mainly at the eyelids owing to the meniscus effect. Jones *et al.*[32] have considered the effect of the lipid layer on the behaviour of a pre-corneal tear film by developing a lubrication model that describes lipid spreading and evolution of tear film thickness. Their results show that the role of lipids is to draw the tear film up the cornea during the opening phase of the blink and that a nonuniform distribution of lipids leads to tear film thinning behind the advancing lipid front.

In the case of contact lens wearers, sufficient amount of post-lens and pre-lens tear film is required in order to maintain the overall health of the eye and to enable proper corrective function of the contact lens. Measurements by Nicholas and King-Smith[33] show that the typical thickness of pre/post-lens tear film is 2.3 μm and that they have different thinning rates.[34] Individuals wearing contact lens may suffer from dry-eye syndrome due to depletion of the post-lens tear film resulting from evaporation of pre-lens tear film[35] or due to increased evaporation and thinning rate of pre-lens tear film and wettability of contact lens.[36]

Recently, Nong and Anderson[37] have described the dynamics and rupture of a pre-lens tear-film, once the eyelid has opened after a blink. In their study, a permeable contact lens is modeled as a fluid saturated porous medium described by the Darcy equations and the pre-lens tear film is assumed to be a layer of incompressible Newtonian fluid over the contact lens and is governed by the Navier-Stokes equations. The lower boundary of the porous layer (lens) is assumed to be impermeable and stationary; this decouples the post-lens film from the model. They have neglected the evaporation of the pre-lens film and have examined the influence of capillarity, gravitational drainage, and contact lens properties such as permeability, thickness of the lens on the dynamics, and rupture of the pre-lens tear film, when the eyelid has opened. A semi-empirical boundary condition (Beavers-Joseph (BJ) condition; Beavers and Joseph[38]) given by $u_y = \frac{\alpha}{\sqrt{K}}(u - u_m)$ has been proposed at the interface along with the conditions of continuity of pressure and mass conservation. Here K is the permeability of the porous medium, α is a dimensionless parameter dependent on the local geometry of the interface of the liquid layer, and the Darcy porous layer, u and u_m are the components of velocity along the substrate in the liquid layer and in the porous medium, respectively. It is to be noted that the BJ condition at the interface allows for a discontinuity in the tangential velocity. Their results using BJ model reveal that the characteristic properties of the porous layer (contact lens) influence the rate of film thinning, but this is not significant for realistic parameter values for contact lens wear. However, the presence of contact lens fundamentally changes the rupture dynamics of pre-lens tear film in the sense that rupture occurs in finite time rather than in infinite time. The results are also presented for Le Bars-Worster slip model,[39] in which the flow variables, namely, velocity and pressure are continuous.

The results of Nong and Anderson[37] are very interesting and significant and motivate one to look for other porous medium models available in the literature to describe the dynamics in the porous layer (contact lens). Such a study would enable one to investigate the influence of other characteristics of the porous layer, such as the porosity of the porous medium (contact lens) on the rate of thinning of the pre-lens tear film and on the dynamics of its rupture.

Goyeau *et al.*[40] and Bousqnet-Melou *et al.*[41] have proposed a model, referred to as the Darcy-Brinkman model for the porous layer, in which the momentum transport in the porous medium accounts for viscous forces and the governing equations are second order partial differential equations. The model accounts for the fluid-fluid viscous interactions that become important very close

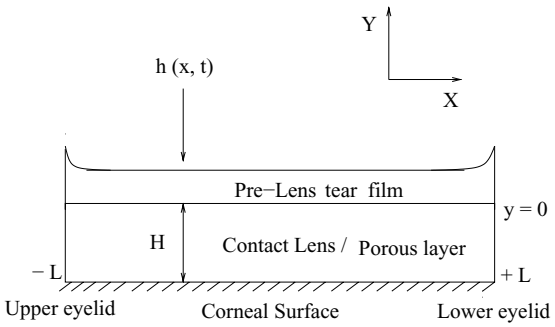

FIG. 1. Schematic diagram for a pre-lens tear film over a contact lens/porous layer model.

to the interface and also ensures continuity of both velocity (normal and tangential components of velocity) and normal stress at the interface. In this model, an interfacial stress-jump condition[42,43] based on the description of the momentum transport at the fluid-porous interface has been proposed. This condition involves a parameter that is related to the spatial changes in the effective properties such as the permeability and the porosity of the porous layer at the interface.[40] It represents a macroscopic description of the momentum transport in a finite mesoscopic interfacial transition layer. It is to be noted that, the use of stress-jump condition at the interface[40,44] amounts to considering a heterogeneous continuously varying transition zone at the interface of the fluid and the porous layers. It is worth mentioning here that this model has been employed by Thiele *et al.*[44] while examining the stability of a thin film flow along a heated inclined porous substrate.

In the present study, a mathematical model is developed to investigate the dynamics of a pre-lens tear film. The pre-lens tear film is assumed to be a thin, viscous incompressible, Newtonian fluid layer with constant viscosity ν and density ρ (aqueous layer) over a permeable contact lens. The contact lens is modeled as a saturated porous medium of constant, finite thickness and is described by the Darcy-Brinkman equations with stress-jump condition at the interface (Fig. 1). The lower boundary of the porous layer (contact lens) is assumed to be impermeable and stationary[37] and this decouples the post-lens tear film from the model. The model incorporates the influence of capillarity, gravitational drainage, contact lens properties such as the permeability, the porosity, and the thickness of the contact lens on the evolution and rupture of a pre-lens tear film, when the eyelid has opened after a blink.

Two models for the evolution of a pre-lens tear film thickness are derived using lubrication theory in Sec. II; the first model incorporates shear-free surface condition at the free-surface while the second model uses tangentially immobile free-surface condition. The second model thus incorporates the effects of the presence of the lipid layer in the form of an imposed boundary condition at the interface of the aqueous and the lipid layers.[13,22] This is reasonably an accurate assumption, once the tear film has been deposited[21] and has been widely used in the investigations on the dynamics of a tear film. Some significant observations and theoretical predictions are presented in Sec. III. The evolution equation for film thickness is numerically solved and the effects of gravity, permeability, porosity, and thickness of the contact lens on the evolution of pre-lens tear film are obtained in Sec. IV. The results are compared with the results of the two slip models derived by Nong and Anderson[37] and the influence of porosity of the contact lens and the viscous-viscous interaction effects at the interface of contact lens and pre-lens tear film are examined.

The results indicate that the presence of permeable contact lens and the characteristics of the contact lens have significant impact on thinning of the pre-lens aqueous layer (long-time behaviour). It is possible to predict tear film break-up times on a contact lens using the results of the present model. It is to be remarked that the present results gain their significance if an individual wearing a contact lens has a longer time between blinks—say on the order of minutes instead of seconds or if one interested in long-time behaviour in a different scenario completely (i.e., not in the tear film context) with a thin fluid film on a porous layer.

II. MATHEMATICAL FORMULATION

Fig. 1 shows a model of a pre-lens tear film as a thin layer of a viscous, incompressible Newtonian fluid over a fluid saturated porous substrate (contact lens). The interface between the pre-lens fluid layer and the porous contact lens is considered to be planar and is located at $y = 0$. As the effect of curvature of the corneal surface on the thinning rate of a tear film (due to the tangential flow in the tear film) is shown to be not significant,[29] the above assumption is justified and the analysis that follows neglects the curvature of the corneal surface. The lower boundary of the porous layer is located at $y = -H$, $H > 0$, and $y = h(x, t)$ defines the free-surface of the pre-lens tear film.

The governing equations in the liquid layer (pre-lens tear film, $0 < y < h(x, t)$) are the Navier-Stokes equations given by

$$u_x + v_y = 0, \tag{1}$$

$$\rho[u_t + uu_x + vu_y] = -p_x + \mu[u_{xx} + u_{yy}] + \rho g \sin\theta, \tag{2}$$

$$\rho[v_t + uv_x + vv_y] = -p_y + \mu[v_{xx} + v_{yy}] - \rho g \cos\theta, \tag{3}$$

where u and v are the two-dimensional velocity components along the x and the y-directions, respectively, p is the pressure, g is the gravity, θ is the angle that the interface at the liquid-porous layer makes with the horizontal. When $\theta = 0$, gravity points in the negative y-direction and $\theta = \pi/2$ corresponds to gravity pointing in the positive x-direction. The flow of liquid in the porous layer is described using the Darcy-Brinkman equations[40,41,45] given by

$$u^b_x + v^b_y = 0, \tag{4}$$

$$\frac{\rho}{\delta}u^b_t = -p^b_x + \mu_e[u^b_{xx} + u^b_{yy}] - \frac{\mu}{K}u^b + \rho g \sin\theta, \tag{5}$$

$$\frac{\rho}{\delta}v^b_t = -p^b_y + \mu_e[v^b_{xx} + v^b_{yy}] - \frac{\mu}{K}v^b - \rho g \cos\theta, \tag{6}$$

where (u^b, v^b) is the filtration velocity vector, K is the permeability, δ is the porosity and μ_e represents the effective viscosity. $\frac{\mu_e}{\mu} = \frac{1}{\delta}$ is the reduced viscosity.[45] The flow in the porous region is assumed to be slow and hence the inertial effects are neglected.[46]

The associated boundary conditions at the free surface $y = h(x, t)$ are the kinematic boundary condition together with the balance of the normal and the shear-stresses and are given by

$$v = h_t + uh_x \quad \text{at} \quad y = h(x, t), \tag{7}$$

$$-p + \frac{2\mu}{(1 + h_x^2)}\left[h_x^2 u_x - u_y h_x - v_x h_x + v_y\right] - \frac{\sigma h_{xx}}{(1 + h_x^2)^{\frac{3}{2}}} = 0 \quad \text{at} \quad y = h(x, t), \tag{8}$$

$$4u_x h_x - (1 - h_x^2)(u_y + v_x) = 0 \quad \text{at} \quad y = h(x, t). \tag{9}$$

Equations (7)–(9) are used to derive the evolution equation for Model I for the shear-free (SF) case. The second model (Model II) is derived using Eqs. (7) and (8) and the condition that the free surface is tangentially immobile given by

$$u + vh_x = 0 \quad \text{at} \quad y = h(x, t). \tag{10}$$

At the liquid-porous interface ($y = 0$),

$$u = u^b \quad \text{at} \quad y = 0, \tag{11}$$

$$v = v^b \quad \text{at} \quad y = 0, \tag{12}$$

$$\mu_e \frac{\partial u^b}{\partial y} - \mu \frac{\partial u}{\partial y} = \frac{\xi}{\sqrt{K}} u^b \quad \text{at} \quad y = 0, \tag{13}$$

$$-p^b + 2\mu_e \frac{\partial v^b}{\partial y} = -p + 2\mu \frac{\partial v}{\partial y} \quad at \quad y = 0. \tag{14}$$

Equation (13) represents the shear-stress jump condition at the liquid-porous interface[42,43] and $\xi \simeq O(1)$. The ideal homogeneous structure of the porous interface corresponds to $\xi = 0$. At the impermeable bottom of the porous layer ($y = -H$),

$$u^b = 0 \quad \text{at} \quad y = -H, \tag{15}$$

$$v^b = 0 \quad \text{at} \quad y = -H. \tag{16}$$

The conditions of fixed film height and fixed film curvature at the lower and the upper lids $x = \pm L$ correspond to the boundary conditions at the ends of the domain and are given by

$$h(\pm L, t) = h^\circ, \tag{17}$$

$$h_{xx}(\pm L, t) = h^\circ_{xx}, \tag{18}$$

where L is the constant half-length of the film (Fig. 1) and h° and h°_{xx} are constants. Following Braun and Fitt,[13] the value of L is taken as $L = 14$ corresponding to the actual dimensional average distance of 1.008 cm between human eyelids and $h^\circ = 9$ and $h^\circ_{xx} = 4$. It is to be noted that the boundary conditions at $x = \pm L$ on the variables in the contact lens (porous layer) need not be prescribed in the present model. It is assumed that in the application of the above boundary conditions, the ends of the contact lens are covered by the eye lids. The initial condition used by Nong and Anderson[37] that models the post-blink geometry of a tear film as a parabolic menisci at the two lids connected to a film with uniform thickness in the interior of the domain is employed in the present study.

The above equations, the initial and the boundary conditions are non-dimensionalized using

$$\bar{x} = \frac{x}{l}, \quad \bar{y} = \frac{y}{d}, \quad \bar{t} = \frac{Ut}{l}, \quad \bar{h} = \frac{h}{d}, \quad \bar{H} = \frac{H}{d},$$

$$\bar{u} = \frac{u}{U}, \quad \bar{v} = \frac{v}{\epsilon U}, \quad \bar{p} = \frac{l\epsilon^2 p}{\mu U}, \quad \bar{u^b} = \frac{u^b}{U}, \quad \bar{v^b} = \frac{v^b}{\epsilon U}, \quad \bar{p}^b = \frac{l\epsilon^2 p^b}{\mu U}, \tag{19}$$

where d is the mean thickness of the film, ϵ is the ratio of the typical vertical to horizontal length scales ($\epsilon = \frac{d}{l}$ and $\epsilon \ll 1$ for tear films), l denotes the characteristic length scale for a surface deformation, and U is the typical velocity scale. The resulting dimensionless equations are given (omitting bars) in the liquid region ($0 < y < h(x, t)$) as

$$u_x + v_y = 0, \tag{20}$$

$$\epsilon^2 Re\left[u_t + uu_x + vu_y\right] = -p_x + \epsilon^2 u_{xx} + u_{yy} + G\sin\theta, \tag{21}$$

$$\epsilon^3 Re\left[v_t + uv_x + vv_y\right] = -\frac{1}{\epsilon} p_y + \epsilon^3 v_{xx} + \epsilon v_{yy} - G\cos\theta, \tag{22}$$

and in the porous layer ($-H < y < 0$) as

$$u^b_x + v^b_y = 0, \tag{23}$$

$$\frac{\epsilon^2 Re}{\delta} u^b_t = -p^b_x + \frac{1}{\delta}[\epsilon^2 u^b_{xx} + u^b_{yy}] + G\sin\theta - \frac{1}{Da} u^b, \tag{24}$$

$$\frac{\epsilon^3 Re}{\delta} v_t^b = -\frac{1}{\epsilon} p_y^b + \frac{1}{\delta}[\epsilon^3 v_{xx}^b + \epsilon v_{yy}^b] - G\cos\theta - \frac{\epsilon}{Da} v^b, \tag{25}$$

and

$$v = h_t + u h_x \ \text{ at } \ y = h(x,t), \tag{26}$$

$$-p + \frac{2\epsilon^2}{\sqrt{1+\epsilon^2 h_x^2}}\left[\epsilon^2 h_x^2 u_x - u_y h_x - \epsilon^2 v_x h_x + v_y\right] = \frac{1}{Ca}\frac{h_{xx}}{(1+\epsilon^2 h_x^2)^{\frac{3}{2}}} \ \text{ at } \ y = h(x,t), \tag{27}$$

$$4\epsilon^2 u_x h_x - (1-\epsilon^2 h^2{}_x)(u_y + \epsilon^2 v_x) = 0 \ \text{ at } \ y = h(x,t) \ \text{ (Model I; SF)}, \tag{28}$$

$$u + \epsilon^2 v h_x = 0 \ \text{ at } \ y = h(x,t) \ \text{ (Model II; TI)}, \tag{29}$$

$$u = u^b \ \text{ at } \ y = 0, \tag{30}$$

$$v = v^b \ \text{ at } \ y = 0, \tag{31}$$

$$u^b = 0 \ \text{ at } \ y = -H, \tag{32}$$

$$v^b = 0, \ \text{ at } \ y = -H, \tag{33}$$

$$\frac{1}{\delta}\frac{\partial u^b}{\partial y} - \frac{\partial u}{\partial y} = \frac{\chi}{\sqrt{Da}} u^b \ \text{ at } \ y = 0, \tag{34}$$

$$-p^b + \frac{2\epsilon^2}{\delta}\frac{\partial v^b}{\partial y} = -p + 2\epsilon^2 \frac{\partial v}{\partial y} \ \text{ at } \ y = 0, \tag{35}$$

where $Ca = \frac{\mu U}{\sigma \epsilon^3}$ is the Capillary number, $Re = \frac{Ul}{\nu}$ is the Reynolds number, $G = \frac{\rho g d^2}{\mu U}$ is the dimensionless gravity parameter, $\chi = \frac{\xi}{\mu}$ is the dimensionless stress-jump coefficient and $Da = \frac{K}{d^2}$ is the Darcy number, representing dimensionless permeability. The porosity δ is not related to the Darcy number and its influence on the pre-lens film dynamics will have to be examined independently of the dimensionless permeability Da.

The dimensionless initial condition is given by

$$h(x,0) = \begin{cases} h_{min}(0), & if\ |x| < \mathrm{L} - \Delta x_m \\ h_{min}(0) + \Delta h_m[|x| - (\mathrm{L} - \Delta x_m)]^2, & if\ |x| > \mathrm{L} - \Delta x_m \end{cases}, \tag{36}$$

where the parameters $h_{min}(0)$, Δh_m, and Δx_m are specified as $h_{min}(0) = 1$ (corresponding to an initial thickness of 10 μm), $\Delta h_m = 2$, and $\Delta x_m = 2$ (Braun and Fitt[13]). Here, Δx_m is the width of the parabolic initial meniscus. Although Δh_m and Δx_m vary from person to person, these values are fixed as above in the following computations as the focus of the present study is to examine the effects of the contact lens (porous layer) properties on the dynamics of a pre-lens tear film. It is to be noted that

$$h_0 = h_{min}(0) + \Delta h_m (\Delta x_m)^2$$

for this choice of initial condition.

Braun and Fitt[13] have chosen the length scale l as $l = (\frac{d\sigma}{\rho g})^{\frac{1}{3}}$ (l denotes the meniscus length; Wilson[47]) and the velocity scale U as $U = \frac{\rho g d^2}{\mu}$. Taking $d = 10$ μm, and using $g = 9.81$ m s^{-2}, $\rho = 10^3$ kg m^{-3}, $\sigma = 0.045$ N m^{-1} (Wong *et al.*[21] and Miller[48]), they get $l = 360$ μm and $U = 755$ μm s^{-1}. As smaller values are suggested by the recent investigations, Winter *et al.*[22] have also examined the cases for $d = 5$ μm ($l = 284$ μm, $U = 189$ μm s^{-1}) and $d = 3$ μm ($l = 240$ μm, U

$= 84\ \mu\text{m s}^{-1}$). The above values of d give rise to time scales $\frac{l}{U}$ as 0.48 s ($d = 10\ \mu$m), 1.5 s ($d = 5\ \mu$m), and 2.9 s ($d = 3\ \mu$m). Also, the above choices for l and U gives $Ca = \frac{\mu U}{\sigma \epsilon^3} = 1$ and $G = 1$.

Taking typical tear film thickness as lying between 1 μm and 5 μm[15,33] and representative contact lens thickness as 100 μm, the ratio of the actual contact lens thickness to a typical tear film thickness ranges between 20 and 100. This ratio is the dimensionless lens thickness H and in the following computations, the above range for H is considered. The chosen values of representative contact lens thickness is based on the studies by Fornasiero *et al.*[35] (water saturated lens; actual thickness 100 μm), Raad and Sabau[49] (actual thickness 300 μm), Maldonado-Codina and Efron[50] (for soft contact lens with actual thickness ranging from 60 to 100 μm) and Monticelli *et al.*[51] (for soft contact lens with actual thickness 200 μm). The contact lens permeability measurements based on the studies by Monticelli *et al.*[51] indicate a value of $10^{-8}\mu\text{m}^2$ approximately. Then, for a range of tear film thickness of 1 μm–5 μm, a realistic value of $Da = \frac{K}{d^2}$ would range between 4×10^{-10} and 4×10^{-8}. Following Raad and Sabau[49] and Nong and Anderson,[37] larger values of Da are considered in the computations to capture the features of the model considered. Therefore, in this investigation, the Darcy number is thus varied from $Da = 0$ for the impermeable case to $Da = 10^{-5}$ based on the ranges of permeability and lens thickness considered.[49,52] Based on the typical value of porosity ($\delta = 0.7$) of the contact lens,[49,53] the porosity is assumed to vary between 0.1 and 0.9. As $\chi \simeq \text{O}(1)$, it is assumed to vary from 0.0 to 0.9.[44]

In what follows, a mathematical model for the evolution of the pre-lens tear film is derived using lubrication approximation of the hydrodynamic equations of motion governing the fluid film, the porous layer, and the boundary conditions. The equations in the thin film limit $\epsilon \ll 1$ are considered by retaining all gravity terms. It is generally assumed[13,54,55] that, when $\theta = \frac{\pi}{2}$, $G \simeq \text{O}(1)$ as $\epsilon \to 0$ and when $\theta = 0$, $\epsilon G \simeq \text{O}(1)$ as $\epsilon \to 0$. As both the scenarios are relevant in the present study, gravity is counted for in both the cases. The system of Eqs. (20)–(35) under the lubrication approximation reduces to

$$u_x + v_y = 0, \tag{37}$$

$$-p_x + u_{yy} + G\sin\theta = 0, \tag{38}$$

$$\frac{1}{\epsilon}p_y + G\cos\theta = 0, \tag{39}$$

in the pre-lens tear film region $0 < y < h(x, t)$ and

$$u^b_x + v^b_y = 0, \tag{40}$$

$$-p^b_x + \frac{1}{\delta}u^b_{yy} + G\sin\theta - \frac{1}{Da}u^b = 0, \tag{41}$$

$$\frac{1}{\epsilon}p^b_y + \cos\theta = 0, \tag{42}$$

in the porous layer region $-H < y < 0$. The boundary conditions are given by

$$v = h_t + uh_x \ \text{ at } \ y = h, \tag{43}$$

$$-p - \frac{1}{Ca}h_{xx} = 0 \ \text{ at } \ y = h, \tag{44}$$

$$u_y = 0 \ \text{ at } \ y = h \ \text{ (Model I; SF)}, \tag{45}$$

$$u = 0 \ \text{ at } \ y = h \ \text{ (Model II; TI)}, \tag{46}$$

$$u = u^b \ \text{ at } \ y = 0, \tag{47}$$

$$v = v^b \text{ at } y = 0, \tag{48}$$

$$u^b = 0 \text{ at } y = -H, \tag{49}$$

$$v^b = 0 \text{ at } y = -H, \tag{50}$$

$$\frac{1}{\delta}\frac{\partial u^b}{\partial y} - \frac{\partial u}{\partial y} = \frac{\chi}{\sqrt{Da}}u^b \text{ at } y = 0, \tag{51}$$

$$p^b = p \text{ at } y = 0. \tag{52}$$

The solution of the above system of Eqs. (37)–(45) and (47)–(52) is given by

$$u = \mathrm{M}(\frac{y^2}{2} - yh) + \mathrm{A}_2, \tag{53}$$

$$v = \frac{\mathrm{M}}{2}y^2 h_x - \mathrm{A}_{2x}y + \mathrm{M}_x(\frac{y^2 h}{2} - \frac{y^3}{6}) + \mathrm{A}_3, \tag{54}$$

$$u^b = \mathrm{C}_1 e^{\sqrt{\frac{\delta}{Da}}y} + \mathrm{C}_2 e^{-\sqrt{\frac{\delta}{Da}}y} - DaM, \tag{55}$$

$$v^b = -\sqrt{\frac{Da}{\delta}}\mathrm{C}_{1x}e^{\sqrt{\frac{\delta}{Da}}y} + \sqrt{\frac{Da}{\delta}}\mathrm{C}_{2x}e^{-\sqrt{\frac{\delta}{Da}}y} - Da\mathrm{M}_x y + \mathrm{B}_3, \tag{56}$$

$$p = p^b = -\epsilon G\cos\theta(y - h) - \frac{1}{Ca}h_{xx}, \tag{57}$$

where

$$\mathrm{A}_2 = \mathrm{C}_1 + \mathrm{C}_2,$$

$$\mathrm{C}_1 = \frac{\mathrm{M}}{\Delta}[Da\mathrm{B}_+ - Da\chi\mathrm{E}_+ - \sqrt{Da}\mathrm{E}_+ h],$$

$$\mathrm{C}_2 = \frac{\mathrm{M}}{\Delta}[Da\mathrm{B}_- + Da\chi\mathrm{E}_- + \sqrt{Da}\mathrm{E}_- h],$$

$$\mathrm{A}_3 = -\mathrm{C}_{1x}\sqrt{\frac{Da}{\delta}}(1 - \mathrm{E}_-) + \mathrm{C}_{2x}\sqrt{\frac{Da}{\delta}}(1 - \mathrm{E}_+) + Da\mathrm{M}_x H, \tag{58}$$

$$\mathrm{B}_3 = \mathrm{C}_{1x}\sqrt{\frac{Da}{\delta}}\mathrm{E}_- - \mathrm{C}_{2x}\sqrt{\frac{Da}{\delta}}\mathrm{E}_+ + Da\mathrm{M}_x\mathrm{H},$$

$$\mathrm{M} = \epsilon\mathrm{G}\cos\theta - \frac{1}{Ca}h_{xxx} - G\sin\theta,\ \Delta = \mathrm{B}_+\mathrm{E}_- + \mathrm{B}_-\mathrm{E}_+,$$

$$\mathrm{B}_+ = \frac{1}{\sqrt{\delta}} + \chi,\ \mathrm{B}_- = \frac{1}{\sqrt{\delta}} - \chi,\ \mathrm{E}_+ = e^{\sqrt{\frac{\delta}{Da}}H},\ \mathrm{E}_- = e^{-\sqrt{\frac{\delta}{Da}}H}.$$

Substitution of (53)–(58) in (43) yields the evolution equation of the pre-lens tear film thickness in the shear free case as (Model I; SF)

$$h_t = \frac{\partial}{\partial x}\Big[\mathrm{M}_{SF}\mathrm{F}_{SF}(h)\Big], \tag{59}$$

where

$$\begin{aligned}
\mathrm{F}_{SF}(h) =& \frac{h^3}{3} + \frac{\sqrt{Da}(\mathrm{E}_+ - \mathrm{E}_-)}{\Delta} h^2 + \frac{2Da}{\sqrt{\delta}} \frac{(\mathrm{E}_+ + \mathrm{E}_- - 2)}{\Delta} h + DaH \\
&+ \frac{2(Da)^{\frac{3}{2}}}{\sqrt{\delta}} \chi \frac{(\mathrm{E}_+ + \mathrm{E}_- - 2)}{\Delta} - \frac{(Da)^{\frac{3}{2}}}{\delta} \frac{(\mathrm{E}_+ - \mathrm{E}_-)}{\Delta}, \\
\mathrm{M}_{SF} =& \epsilon G \cos\theta - \frac{1}{Ca} h_{xxx} - G \sin\theta.
\end{aligned} \tag{60}$$

The model consisting of Eqs. (59) and (60), the initial condition (Eq. (36)) and the non-dimensional boundary conditions (Eqs. (17) and (18)) describe the evolution of post-blink pre-lens tear film in the shear-free case. For an individual standing in the upright position ($\theta = \frac{\pi}{2}$), the evolution equation (64) with $Ca = 1$ and $G = 1$ reduces to that obtained by Braun and Fitt[13] for the no evaporation case.

The equation describing the evolution of pre-lens tear film using the tangentially immobile condition (Eq. (46)) at the free surface (Model II) is obtained (the Appendix) and is given by (Model II; TI).

$$h_t = \frac{\partial}{\partial x}\Big[\mathrm{M}_{TI}\mathrm{F}_{TI}(h)\Big], \tag{61}$$

where

$$\begin{aligned}
\mathrm{F}_{TI}(h) =& \frac{h^3}{12} + \frac{\sqrt{Da}}{4} \frac{(\mathrm{E}_+ - \mathrm{E}_-)}{\Delta'} h^3 + \frac{Da}{\sqrt{\delta}} \frac{(\mathrm{E}_+ + \mathrm{E}_- - 2)}{\Delta'} h^2 + \frac{2(Da)^{\frac{3}{2}}}{\sqrt{\delta}} \chi \frac{(\mathrm{E}_+ + \mathrm{E}_- - 2)}{\Delta'} h \\
&- \frac{(Da)^{\frac{3}{2}}}{\delta} \frac{(\mathrm{E}_+ - \mathrm{E}_-)}{\Delta'} h + DaH - \frac{2Da^2}{\sqrt{\delta}} \frac{(\mathrm{E}_+ + \mathrm{E}_- - 2)}{\Delta'}, \\
\Delta' =& h\Delta + \sqrt{Da}(\mathrm{E}_+ - \mathrm{E}_-), \\
\mathrm{M}_{TI} =& \epsilon G \cos\theta - \frac{1}{Ca} h_{xxx} - G \sin\theta.
\end{aligned} \tag{62}$$

In the absence of a porous layer (no contact lens), the Eqs. (59)–(62) reduce to

$$\frac{\partial h}{\partial t} = \frac{\partial}{\partial x}\Big[\frac{h^3}{3}(\epsilon G \cos\theta - G \sin\theta - \frac{1}{Ca} h_{xxx})\Big], \tag{63}$$

$$\frac{\partial h}{\partial t} = \frac{\partial}{\partial x}\Big[\frac{h^3}{12}(\epsilon G \cos\theta - G \sin\theta - \frac{1}{Ca} h_{xxx})\Big], \tag{64}$$

respectively. When gravity is neglected in Eq. (63), the evolution equation derived for a film over an impermeable substrate is recovered.[56] Also, when $\epsilon G\cos\theta$ term is neglected in Eq. (63), it reduces to the equation derived by Hocking,[57] in which the sliding and spreading of two dimensional time-dependent motion of a thin drop placed on an inclined plane has been examined within the frame work of lubrication theory.

It is observed from Eqs. (60) and (62) that the terms appearing in $\mathrm{F}_{SF}(h)$ and $\mathrm{F}_{TI}(h)$ are polynomials in h and the coefficients of h^r, $r = 0, 1, 2$ are constants that scale as some power of dimensionless length, say l_{os}, where $l_{os} = \frac{\sqrt{Da}(\mathrm{E}_+ - \mathrm{E}_-)}{\mathrm{B}_+\mathrm{E}_- + \mathrm{B}_-\mathrm{E}_+}$. If l_{os} is assumed to be small so that $\mathrm{O}({l_{os}}^2)$ can be neglected in $\mathrm{F}_{SF}(h)$ and $\mathrm{F}_{TI}(h)$, then Eqs. (59) and (61) reduce to

$$\frac{\partial h}{\partial t} + \frac{\partial}{\partial x}\Big[\mathrm{M}_{SFOS}\mathrm{F}_{SFOS}(h)\Big] = 0; \quad \mathrm{F}_{SFOS}(h) = \frac{h^3}{3} + l_{os}h^2 \tag{65}$$

for the shear-free case (one-sided model) and

$$\frac{\partial h}{\partial t} + \frac{\partial}{\partial x}\left[\frac{\mathrm{M}_{TIOS}}{4}\mathrm{F}_{TIOS}(h)\right] = 0; \quad \mathrm{F}_{TIOS}(h) = \frac{h^3}{3} + \frac{l_{os}h^3}{h + l_{os}} \tag{66}$$

for the tangentially immobile free-surface case (one-sided model). Here $\mathrm{M}_{SFOS} = \mathrm{M}_{TIOS} = \mathrm{M}_{SF} = \mathrm{M}_{TI}$. Comparing Eq. (65) with the evolution equation for the one-sided slip model derived by Sadiq and Usha,[58] it is observed that the terms in F_{SFOS} in Eq. (65) are identical with the highest order truncation of the evolution equation presented by Sadiq and Usha[58] and subsequently by Thiele *et al.*[44] (equation C_6 in Appendix B of Thiele *et al.*[44] paper), with slip length identified with l_{os}. The one-sided slip models described by Eqs. (65) and (66) suggest that when the permeability of the porous medium is low, then one can effectively replace the porous layer by a slip condition at a smooth solid substrate with slip parameter l_{os} defined as above.

III. FURTHER OBSERVATIONS AND THEORETICAL PREDICTIONS

The evolution equations (59) and (61) have terms proportional to h^3, h^2, h, and terms independent of h. These equations resemble the equation $h_t + Q_x = 0$, analyzed both theoretically and numerically by Bertozzi *et al.*[59] and Bertozzi,[60] where $Q = -h^n h_{xxx}$. The details of singularity formation and film rupture predicted by their investigations are presented in Table I for pressure boundary conditions given by $h(\pm 1) = 1$, $h_{xx}(\pm 1) = m$, where m is a given constant. Their results[59,60] (Table I) reveal that for $m > 2$, a solution h to $h_t + Q_x = 0$ satisfying the above pressure boundary conditions and smooth initial condition would always go to zero in either finite or infinite time.

In the present investigation, the boundary conditions at $x = \pm L$ are analogous to that in Bertozzi *et al.*[59] and Bertozzi.[60] with $m = \frac{4(14)^2}{9} \simeq 87 > 2$. Also, as $h \to 0$ in Eqs. (59), (61), (65), and (66), it is observed that $\mathrm{F}_{SF}(h)$, $\mathrm{F}_{TI}(h)$, $\mathrm{F}_{SFOS}(h)$, and $\mathrm{F}_{TIOS}(h)$ tend to h^n, where n takes values 0 or 2 or 3. Table II presents the details and description of the model equations in the present study for the different cases. The expected behaviour of the models for different cases presented in Table II is inferred from the predictions by Bertozzi *et al.*[59] and Bertozzi,[60] given in Table I.

It is to be noted that the new features of the present model have made predictions that are different from Nong and Anderson's[37] model for the case $Da \neq 0$, $H = 0$, which corresponds to a pre-lens film over a porous contact lens with no thickness. Examining the evolution equations, Eq. (59) (Model I: SF) and Eq. (61) (Model II: TI), it is observed that, $Da \neq 0$, $H = 0$ gives $E_+ = E_- = 1$ and therefore $E_+ - E_- = 0$ and $E_+ + E_- - 2 = 0$. The constant terms in $\mathrm{F}_{SF}(h)$ in Eq. (59) and $\mathrm{F}_{TI}(h)$ in Eq. (61) vanish and $\mathrm{F}_{SF}(h) \to h^n$, and $\mathrm{F}_{TI}(h) \to h^n$ as $h \to 0$. In both the models, the exponent n takes the value 3.

Further, this case ($Da \neq 0$, $H = 0$) can be thought of as describing the one-sided model (in which the flow in the porous layer is not accounted for) of a pre-lens film over a porous contact lens with no thickness. It is with this in view, the one-sided models are derived and presented in Eq. (65) for the shear-free case and Eq. (66) for tangentially immobile case. Note that $l_{os} = 0$ when $Da \neq 0$, $H = 0$. This again yields $\mathrm{F}_{SFOS}(h) \to h^n$, and $\mathrm{F}_{TIOS}(h) \to h^n$ as $h \to 0$, where the exponent n takes the value 3.

TABLE I. Details of singularity formation in $h_t + (h^n h_{xxx})_x = 0$ predicted by Bertozzi *et al.*[59] and Bertozzi.[60]

n	Finite-time singularities (singular rupture behaviour, $h \to 0$)	Infinite-time singularities
$n \geq 4$		✓
$n \geq 2$, h_{xx} bounded		✓
$0 \leq n \leq 1.2$	✓	
$n > 0.75$		✓
Small n	✓	

TABLE II. Details and description of model equations of the present study.

S. no	Details				Description	Expected behaviour
1	Eqs. (59) and (60)	$Da \neq 0$	$H \neq 0$ $\chi = 0$ or $\chi \neq 0$	$n = 0$	A thin film over a permeable contact lens with finite thickness and either zero or non zero stress-jump coefficient for a shear-free surface	Finite-time singularity
2	Eqs. (61) and (62)	$Da \neq 0$	$H \neq 0$ $\chi = 0$ or $\chi \neq 0$	$n = 0$	A thin film over a permeable contact lens with finite thickness and either zero or non zero stress-jump coefficient for a tangentially immobile free surface	Finite-time singularity
3	Eqs. (59) and (60)	$Da = 0$	$H = 0$	$n = 3$	A film over an impermeable substrate (precorneal tear film) with no slip; a film over an impermeable contact lens (with finite thickness) with shear-free surface	Infinite-time singularity infinite-time singularity
4	Eqs. (61) and (62)	$Da = 0$	$H = 0$ $H \neq 0$	$n = 3$	A film over an impermeable substrate (precorneal tear film) with no slip; a film over an impermeable contact lens (with finite thickness) with tangentially immobile free surface.	Infinite-time singularity infinite-time singularity

The two-sided and the one-sided models predict the same conclusions for the case $Da \neq 0$, $H = 0$ as $h \to 0$. As the exponent n takes the value $n = 3$, the dynamics for the pre-lens tear film over a porous contact lens with no thickness can be expected to exhibit infinite-time singularity, in accordance with the theory of Bertozzi *et al.*[59,60] However, this is not so for the case $Da \neq 0$, $H = 0$ with models presented by Nong and Anderson.[37]

It is clear from the above discussion that the new features (porosity, stress-jump parameter) incorporated in the present models have helped in predicting the dynamics and rupture in this case.

It is also inferred from Table II that one can expect finite-time singularity (rupture) to occur in the case of a tear film over a contact lens of finite thickness H (however small H may be). Such a finite time singularity occurs due to the presence of the constant terms in both the two-sided models ($Da \neq 0$, $H \neq 0$; Eqs. (59) and (60) for the shear-free case and Eqs. (61) and (62) for the tangentially immobile case).

Further, the other characteristics of the porous medium, namely, the porosity δ and the stress-jump coefficient also play a role in the rate of thinning of the pre-lens tear film and these aspects are examined through the numerical solution of the evolution equation for pre-lens tear film thickness.

IV. NUMERICAL RESULTS AND DISCUSSIONS

The method of lines approach is employed to solve the evolution equations for the shear-free case (Eqs. (59) and (60)) and for the tangentially immobile case (Eqs. (61) and (62)) numerically. The spatial derivatives are discretized using second-order accurate conservative finite difference scheme (applied at $N + 1$ equally spaced points $x_j = -L + 2L(j - 1)/N$, $j = 1, 2, \ldots N + 1$) and a system of ODE for $h_j(t) = h(x_j, t)$ is generated for a set of parameter values estimated for realistic properties of contact lens and tear film. A backward difference time stepping is used and this ensured that the method is stable and efficient. The computations are performed for sufficiently large dimensionless times in order to understand and predict long-time scenarios in the dynamics of pre-lens tear film for an individual wearing the contact lens. The numerical computations are stopped when the value of h is less than a single grid spacing; and the time at which this happens is taken as the tear film break-up time; namely, the time taken for a dry patch to appear on the surface of the lens. The system is solved using MATLAB *ode*15*s* solver and the computations are carried out for $-L \leq x \leq L$ (with $L = 14$, which corresponds to a dimensionless distance between the eyelids of 1.008 cm) with $h(x = \pm L) = h^{\circ}$ and $h_{xx}(x = \pm L) = h^{\circ}_{xx}$. The results obtained with the number of spatial grid points $N = 2000$ provided sufficient accuracy and no significant change in the results is observed for any N beyond 2000.

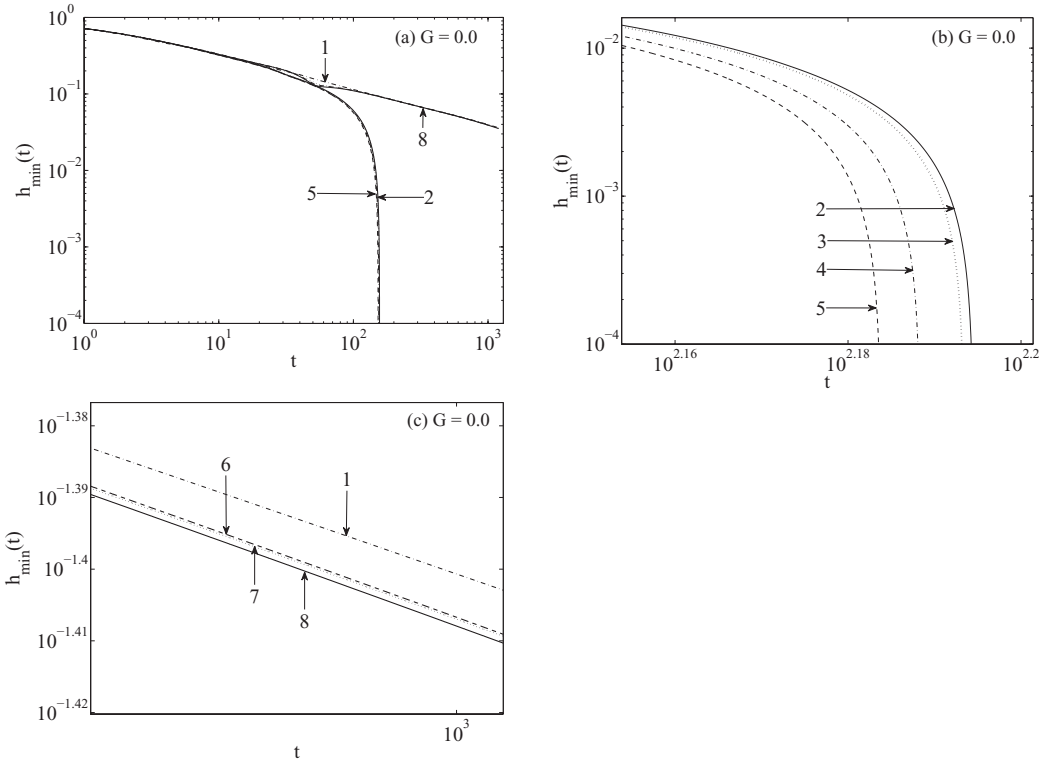

FIG. 2. (a) Minimum pre-lens tear film thickness h_{min} as a function of time t in the absence of gravity. $H = 100$ for all curves except (1). (b) The magnification of h_{min} within the interval $10^{2.15} < t < 10^{2.2}$ in Fig. 2(a). (c) The magnification of h_{min} within the interval $10^{2.966} < t < 10^{3.005}$ in Fig. 2(a). 1. $Da = 0$, $H = 0$ (Fig. 2(c)). 2. $Da = 10^{-5}$, $\delta = 0.1$, $\chi = 0.0$ (Fig. 2(b)). 3. $Da = 10^{-5}$, $\delta = 0.1$, $\chi = 0.4$ (Fig. 2(b)). 4. $Da = 10^{-5}$, $\delta = 0.5$, $\chi = 0.4$ (Fig. 2(b)). 5. $Da = 10^{-5}$, $\delta = 0.5$, $\chi = 0.75$ (Fig. 2(b)). 6. $Da = 10^{-8}$, $\delta = 0.1$, $\chi = 0.0$ (Fig. 2(c)). 7. $Da = 10^{-8}$, $\delta = 0.1$, $\chi = 0.4$ (Fig. 2(c)). 8. $Da = 10^{-8}$, $\delta = 0.5$, $\chi = 0.75$ (Fig. 2(c)).

In order to validate the results of the present numerical code with the results of the previous investigations, solutions are computed for $Da = 0$, $H = 0$, $G = 0$, and $Ca = 4$ and they agreed with the numerical solution presented in Fig. 2 of Braun and Fitt[13] on the pre-corneal tear film drainage after a blink (see Fig. 2).

In what follows, the results are presented when an individual, wearing a contact lens, is standing in the upright position ($\theta = \pi/2$). Also, a non-dimensional time of 2.08 corresponds to 1s. Figs. 2(a)–2(c) show the effects of the presence of the porous layer/contact lens on the minimum pre-lens film thickness in the shear-free case (solution of Eqs. (59) and (60)), when the gravity effects are neglected. The drainage of the film occurs due to capillary forces. The results for $Da = 10^{-8}$, $H = 100$ (curves 6, 7, 8) and $Da = 10^{-5}$, $H = 100$ (curves 2, 3, 4, 5) are presented along with the results for $Da = 0$ and $H = 0$ (curve 1). The stress-jump coefficient χ takes values $\chi = 0.0, 0.4$, and 0.75 while δ takes values $\delta = 0.1$ and 0.5. The results are computed for Ca = 4.

The results for $Da = 10^{-8}$ and $H = 100$ (curve 6, $\delta = 0.1$, $\chi = 0.0$, not shown in Fig. 2(a) but shown in Fig. 2(c)) for a pre-lens tear film over a permeable thick contact lens is very close to the results for $Da = 0$, $H = 0$ (curve 1), which corresponds to the case of a pre-corneal tear film (Braun and Fitt;[13] no gravity, no evaporation case) for time scales close to 400. This trend is also observed in the results by Nong and Anderson[37] where porosity effects are not incorporated. This shows that the presence of the contact lens with small permeability, small porosity, and zero stress-jump coefficient (which corresponds to ideal, homogeneous structure of the interface between the contact lens and tear film) has no significant influence on the thinning dynamics of the pre-lens tear film for these time scales. That is, when Da is very small, at this time scale, the frictional forces are strong enough to resist the thinning of the film.

However, for time scales beyond dimensionless time t = 400, there are quantitative differences (curve 1 and curve 6) as shown in Fig. 2(c) (magnification of the results in Fig. 2(a) in the interval $10^{2.966} < t < 10^{3.005}$). Although the permeability and the porosity are very small, ($Da = 10^{-8}$, $\delta = 0.1$), their influence is to thin down the pre-lens tear film and this is clearly seen in Fig. 2(c). At these time scales, even for this mild change in porosity, the viscous-viscous interaction begins to play its role. As the stress-jump coefficient is slightly increased to $\chi = 0.4$ (which accounts for spatial heterogeneity of the interfacial region, curve 7 in Fig. 2(c)), no significant thinning occurs even at these time scales (curve 6 and curve 7). However, an increase in porosity δ to $\delta = 0.5$ and stress-jump coefficient to $\chi = 0.75$ (curve 8 in Fig. 2(c)) results in slight decrease in the thickness of the pre-lens tear film (curves 6, 7 and curve 8).

Still for this case, for which $Da \neq 0$, $H \neq 0$, there are no signs of occurrence of finite-time rupture close to this time scale, as predicted by the theory in Bertozzi *et al.*[59,60] and presented in Table II. This may be due to the smallness of the $n = 0$ term in Eqs. (59) and (60) as compared to the order of magnitude of the $n = 3$ term at this time scale for the values of permeability, porosity, and stress-jump coefficient considered. It may be remarked that the results of Bertozzi *et al.*[59] show a $t^{-0.5}$ thinning rate at the end of the domain. This result is for asymptotically long time. It is applicable for the thinning dynamics of a film for the capillary-pressure driven case and not for the thinning rate of a tear film. Therefore, it may not be possible to achieve this result in tear film conditions where a typical inter blink time is approximately 10 s.

As the permeability of the contact lens increases to $Da = 10^{-5}$, the contribution from the $n = 0$ term in Eqs. (59) and (60) becomes significant even at dimensionless time scales close to $t = 40$ (Fig. 2(a)) and for the values of the parameters chosen. This is evident from the enhancement in the thinning rate of the pre-lens tear film (curves 2, 5 in Fig. 2(a) and curves 2-5 in Fig. 2(b)) (magnification of Fig. 2(a) for the interval $10^{2.15} < t < 10^{2.2}$). At this value of $Da = 10^{-5}$, the influence of χ and δ are clearly visible from Fig. 2(b). An increase in porosity δ (curves 3 and 4; $\chi = 0.4$) increases the rate of thinning as seen in Fig. 2(b) and a further increase in χ to $\chi = 0.75$ (curve 5 in Fig. 2(b)) enhances the thinning rate of the film. In fact, an increase in porosity $\delta(\frac{\mu_e}{\mu} = \frac{1}{\delta})$ corresponds to a decrease in the effective viscosity μ_e in the porous layer. As a result, there is a decrease in the resistance offered by the frictional forces to the thinning of the film. Hence, there is an increase in the thinning rate and advancement in finite-time rupture. Also, $\chi = 0$ (stress-jump parameter) corresponds to continuity of shear stresses at the interface of the porous layer and the pre-lens tear film. An increase in the stress-jump parameter χ gives rise to an increase in the relative jump in the shear stress at the interface of the porous medium and the pre-lens tear film. So, in this case, the frictional forces that arise due to viscous-viscous interaction which is accounted for in the present model, are not sufficient enough to offer resistance to thinning and hence the rate of thinning increases and advances the finite-time rupture. It is also observed that, in consistency with the results of Bertozzi *et al.*[59] and Bertozzi,[60] finite-time rupture occurs at this Da value ($Da = 10^{-5}$). The life-span of a pre-lens tear film over a contact lens with larger porosity and spatially heterogeneous interface is shorter (curve 5 in Fig. 2(b)) as compared to a film over a contact lens with smaller porosity with an ideal homogeneous interface (curve 2 in Fig. 2(b)).

The corresponding results for minimum pre-lens tear film thickness, by incorporating the gravity effects ($G = 0.25$) are presented in Fig. 3(a) for the shear-free case with $Ca = 4$. The capillary force, the gravitational force and the frictional forces that arise due to viscosity are responsible for drainage of pre-lens tear film. The long-time scenarios are presented for different values of the parameters so as to clearly see the effects of gravity. It is observed that gravity has no significant effect on thinning dynamics for time scales close to 100 at small values of permeability ($Da = 10^{-8}$; curves 6, 7, and 8, Fig. 3(a)). But, beyond this dimensionless time, the pre-lens tear film thins down significantly due to the effects of gravity (Fig. 3(a)) and film rupture occurs in finite-time in accordance with the theory of Bertozzi *et al.*[59] (compare the results of Figs. 3(a) and 2(a) for the corresponding parameter values). This may be due to the fact that beyond a dimensionless time of 10^3, the constant term in Eqs. (59) and (60) dominates and thus contributes to the change in the dynamics of the thinning of the film. The magnification of the results in the interval $10^{3.823} < t < 10^{3.841}$ in Fig. 3(a) for the curve 1 ($Da = 0$, $H = 0$) and the curves 6, 7, and 8 ($Da = 10^{-8}$, $H = 100$) are presented in Fig. 3(b). The results show that, an increase in porosity δ and an increase in χ advance the rupture of

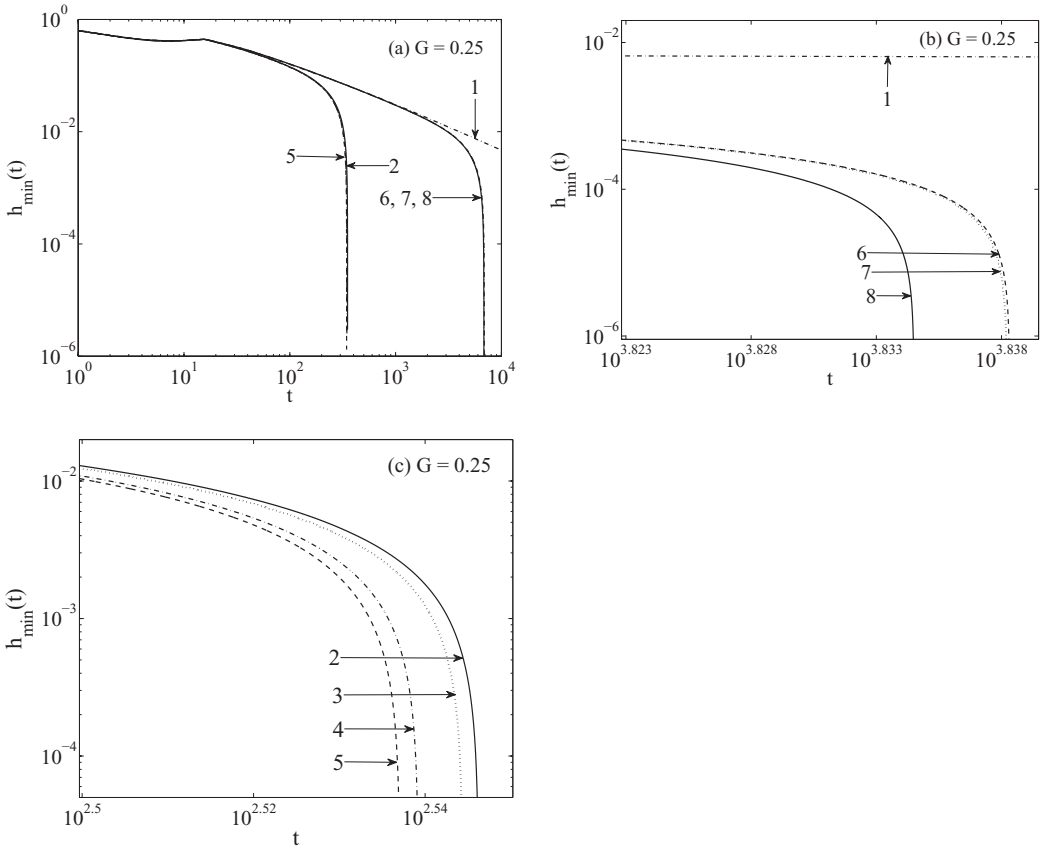

FIG. 3. (a) Minimum pre-lens tear film thickness h_{min} as a function of time t in the presence of gravity. $H = 100$ for all curves except (1). (b) The magnification of h_{min} within the interval $10^{3.823} < t < 10^{3.841}$ in Fig. 3(a). (c) The magnification of h_{min} within the interval $10^{2.5} < t < 10^{2.55}$ in Fig. 3(a). 1. $Da = 0$, $H = 0$ (Fig. 3(b)). 2. $Da = 10^{-5}$, $\delta = 0.1$, $\chi = 0.0$ (Fig. 3(c)). 3. $Da = 10^{-5}$, $\delta = 0.1$, $\chi = 0.4$ (Fig. 3(c)). 4. $Da = 10^{-5}$, $\delta = 0.5$, $\chi = 0.4$ (Fig. 3(c)). 5. $Da = 10^{-5}$, $\delta = 0.5$, $\chi = 0.75$ (Fig. 3(c)). 6. $Da = 10^{-8}$, $\delta = 0.1$, $\chi = 0.0$ (Fig. 3(b)). 7. $Da = 10^{-8}$, $\delta = 0.1$, $\chi = 0.4$ (Fig. 3(b)). 8. $Da = 10^{-8}$, $\delta = 0.5$, $\chi = 0.75$ (Fig. 3(b)).

a pre-lens tear film, in the presence of gravity. The same trend is observed for $Da = 10^{-5}$ (Fig. 3(c); magnification of the results in the interval $10^{2.5} < t < 10^{2.55}$ in Fig. 3(a) for the curves 2, 3, 4, and 5). Also, an increase in permeability enhances the film thinning and shortens the life span of pre-lens tear film for fixed values of other characteristics of the lens (Figs. 3(a) and 3(c)). When $Da = 10^{-5}$, it is inferred from Figs. 2(a) and 3(a) that the life span of a tear film over a contact lens increases due to the effects of gravity in the sense that the rupture time is close to 400 non-dimensional time when gravity is active in comparison to 150 non-dimensional time in the absence of gravity. The results show (Fig. 3(a)) that minimum film thickness occurs at the bottom of the tear film (closer to the lower eyelid) at early times; but due to the effects of gravity, there is a transition occurring during the non-dimensional time $t = 10$ and $t = 20$ and tear film begins to thin in the region closer to the upper eyelid.

Fig. 4(a) presents the evolution of pre-lens tear film for $Da = 10^{-5}$, $H = 100$, $\delta = 0.5$, $\chi = 0.75$, while Fig. 4(b) presents the results for $Da = 10^{-8}$ with other parameters as above. In the case when the gravity effects are neglected (Fig. 4(a), $G = 0$), the thickness of the pre-lens tear film is symmetrical about $x = 0$ (dotted curve; $G = 0$, $t = 150$). There is a steep decrease in the thickness of the film closer to the ends of the domain and around $x = \pm 12$, the film thickness reaches its minimum. This trend is also observed by Wong *et al.*,[21] Braun and Fitt,[13] and Nong and Anderson.[37] There is no region where the curvature of the tear film evolution is zero; however, it is very small in

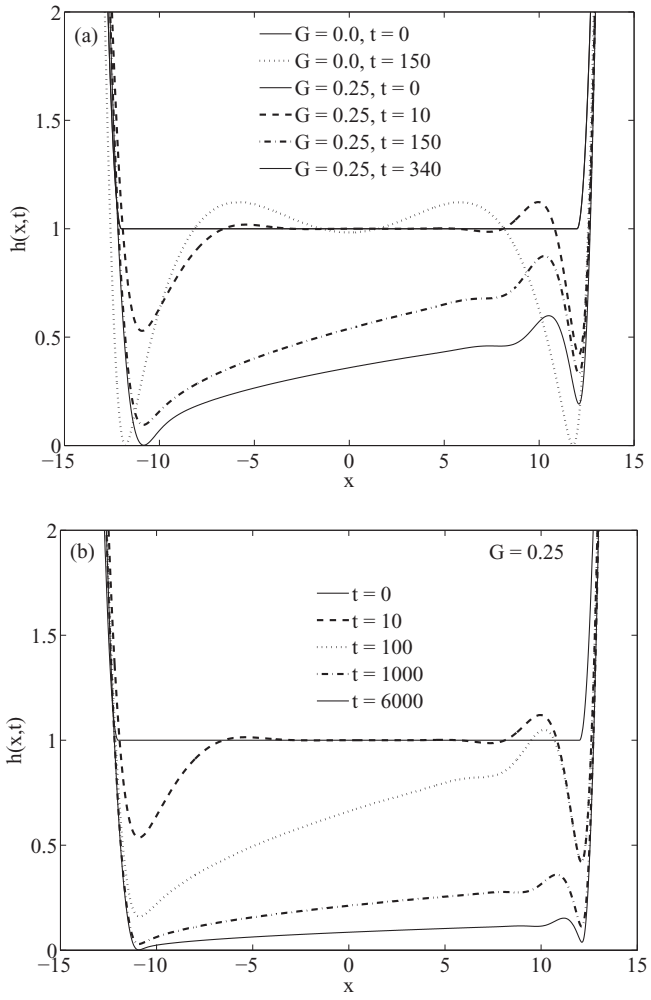

FIG. 4. Pre-lens tear film profiles at different times when $H = 100$, $\delta = 0.5$, $\chi = 0.75$. (a) $Da = 10^{-5}$. (b) $Da = 10^{-8}$.

the interior of the domain away from the menisci. The evolution of the tear film is such that there is a thickening of the film symmetrically on either side of $x = 0$.

When the gravity effects are included (Fig. 4(a), $Da = 10^{-5}$ and Fig. 4(b), $Da = 10^{-8}$), the film loses its symmetry about $x = 0$. At early times, the minimum film thickness occurs at the bottom of the eye ($x = L$) (curve for $t = 10$ in Fig. 4(a); curve for $t = 10$ in Fig. 4(b)). As time progresses, the gravitational drainage dominates and minimum film thickness occurs near the top of the eye $x = -L$. Due to the effect of gravity, the regions close to the upper lid thin down more than the regions close to the lower lid. Gravity drives the tear film flow in the positive x-direction and distributes the film from top to the bottom of the lens. The flow of the tear film is observed in the entire domain. The evolution of film thickness as well as the thinning rate are influenced by the effects of gravity.

It is clear that capillary and gravitational forces balance each other and this causes a change in the film thickness shape at the lower lid $x = L$. On the other hand, the region away from the menisci is dominated by gravity. The viscous, capillary, and gravity effects become important close to the lower lid where the film thickness assumes a wave like shape resembling a "tear pool" (Figs. 4(a) and 4(b), $G = 0.25$). It is to be noted that such a tear pool is not observed in the case when gravity effects are excluded (Fig. 4(a)). When gravity effects are included, film rupture always takes place closer to the upper part of the domain. The effects of contact lens characteristics on the evolution of pre-lens tear film are presented later.

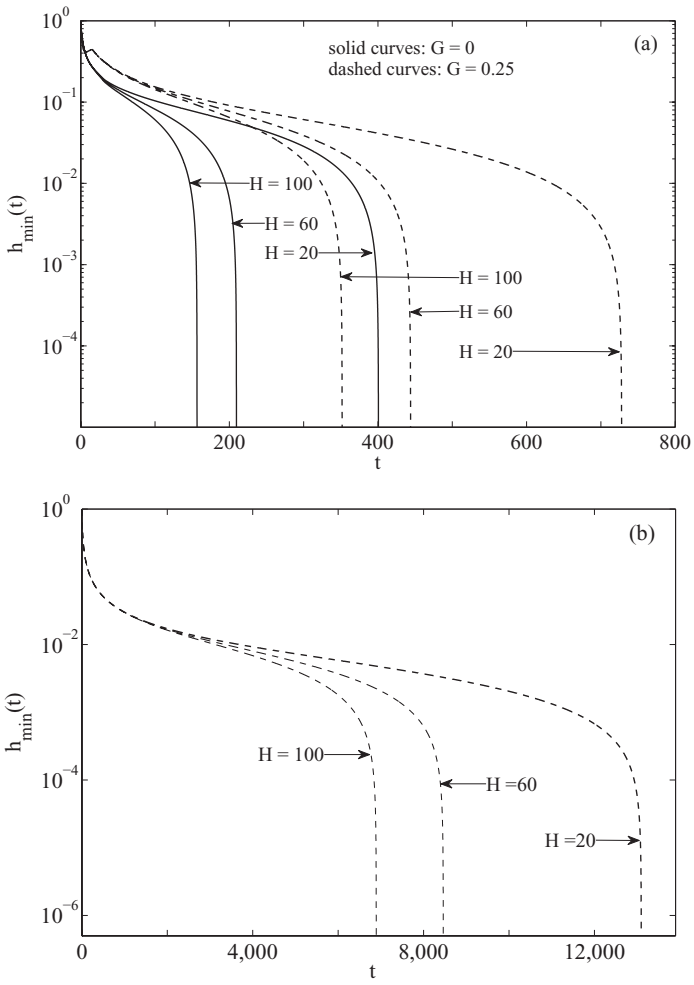

FIG. 5. Effects of thickness (H) of the porous substrate and gravity on the minimum film thickness h_{min} when $\delta = 0.1$, $\chi = 0$. (a) $Da = 10^{-5}$; (b) $Da = 10^{-8}$, $G = 0.25$.

The influence of contact lens thickness on the rate of thinning of pre-lens tear film and rupture dynamics are assessed when $Da = 10^{-5}$ (Fig. 5(a)) and $Da = 10^{-8}$ (Fig. 5(b)), for $\delta = 0.1$, $\chi = 0.0$. The solid curves correspond to the results with no gravity effects while the dashed curves are for the case when gravity is active. At early times, the contact lens thickness has negligible effect on the rate of thinning of the film. Beyond non-dimensional time $t = 20$, the rate of thinning of the film increases with an increase in the thickness of the contact lens. This is so, in the presence or absence of effects of gravity (Fig. 5(a), $Da = 10^{-5}$). In the absence of gravity, rupture of the pre-lens tear film occurs earlier and for an individual wearing a thick contact lens, the life span of vertical pre-lens tear film is shorter (Fig. 5(a)). However, gravity helps to slow down the rupture of pre-lens tear film (Fig. 5(a)). The same trend is observed as the permeability Da is decreased (Fig. 5(b)). The results show that when porosity is small, the thicker the contact lens, the shorter is the life time of the pre-lens tear film, for the chosen values of the parameters.

It is of interest to observe the evolution of the pre-lens tear film over a thinner contact lens ($H = 20$), when gravity is active and assess the influence of porosity of the lens (Fig. 6(a)) and the effects of stress-jump parameter (Fig. 6(b)) on the rate of thinning of the pre-lens tear film. The pre-lens tear film shape at $t = 670$ (non-dimensional) is shown in Fig. 6(a) for $\chi = 0.75$ and in Fig. 6(b) for $\delta = 0.5$. As rupture occurs closer to the upper lid due to the effects of gravity, the magnification of the results closer to the upper lid are presented as an inset in Figs. 6(a) and 6(b) for different δ values and different χ values, respectively. The insets in Figs. 6(a) and 6(b) show that pre-lens

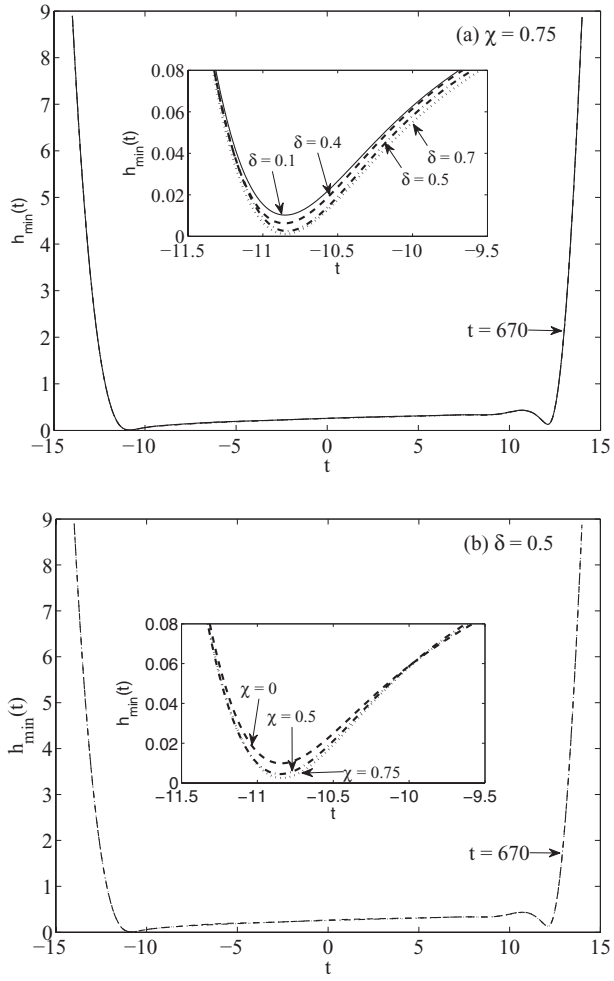

FIG. 6. Pre-lens tear film shape at $t = 670$ on a contact lens for $H = 20$, $G = 0.25$, $Da = 10^{-5}$. (a) Influence of porosity δ on the evolution of the film when $\chi = 0.75$ (b) Influence of stress-jump coefficient χ when $\delta = 0.5$.

tear film thickness is a monotonic decreasing function of δ (porosity of the lens) (Fig. 6(a)) and χ (stress-jump parameter) (Fig. 6(b)) for the chosen values of other parameters.

In order to understand the effects of δ, χ, and H on rupture time, the computations are carried out and the details are presented in Table III for different values of δ, $\chi = 0.75$, $G = 0.25$ and Table IV for different values of χ, $\delta = 0.5$, $G = 0.25$. The results reveal that the life span of a pre-lens tear film is longer on a thinner contact lens for all the values of porosity and permeability considered. The rupture time is a monotonic decreasing function of δ as well as of χ for any thickness of the contact lens (Tables III and IV). As the permeability increases, the rupture time is very much advanced. While the decrease in the rupture time for contact lens with same porosity is significant

TABLE III. Rupture time when $G = 0.25$, $\chi = 0.75$.

$\chi = 0.75$	$Da = 10^{-8}$							$Da = 10^{-5}$						
$\delta \rightarrow$	0.1	0.2	0.3	0.4	0.5	0.6	0.7	0.1	0.2	0.3	0.4	0.5	0.6	0.7
$H = 20$	13080	13050	13000	12960	12900	12860	12790	734	729.2	714.8	714.4	698.8	695.6	681.5
$H = 60$	8456	8438	8418	8396	8381	8359	8326	447.2	443.2	438.9	435.0	430.4	427.8	422.2
$H = 100$	6895	6874	6861	6846	6831	6812	6793	353.0	350.1	349.0	346.9	344.4	340.5	338.1

TABLE IV. Rupture time when $G = 0.25$, $\delta = 0.5$.

$\delta = 0.5$	$Da = 10^{-8}$								$Da = 10^{-5}$							
$\chi \rightarrow$	0	0.1	0.2	0.3	0.4	0.5	0.6	0.75	0	0.1	0.2	0.3	0.4	0.5	0.6	0.75
$H = 20$	13040	13020	13010	13000	12990	12970	12950	12900	720.5	721.1	717.3	714.1	709.4	705.6	704.3	698.8
$H = 60$	8437	8431	8427	8426	8411	8406	8395	8381	441.4	440.8	439.2	439.1	437.6	436.6	433.8	430.4
$H = 100$	6872	6870	6867	6865	6865	6851	6845	6831	350.0	348.4	348.2	347.4	346.3	345.6	345.4	344.4

as the thickness of the contact lenses increases, this is not so for contact lenses with same thickness but varying porosity. The decrease in rupture time for contact lenses with same thickness but varying stress-jump parameter χ is not as significant as that for contact lenses with the same χ but increasing thickness. The rupture time is highly influenced by the combined effects of porosity and the thickness of contact lens. The higher order Darcy-Brinkman model used to describe the dynamics of pre-lens tear film, incorporating the important characteristics such as porosity, permeability, thickness of the contact lens, and stress-jump parameter predicts finite-time break-up. It is possible to explain the mechanism that is responsible for the above features exhibited by the characteristics of the porous contact lens and the resulting dynamics of pre-lens tear film.

Porosity is a geometric property of the porous contact lens and is a measure of the fluid storage capacity of the contact lens. An increase in porosity would result in the flow of tear film in the direction from the film towards the porous contact lens. This results in faster thinning of the pre-lens tear film. Also, as porosity δ increases, the effective viscosity in the porous layer μ_e ($\frac{\mu_e}{\mu} = \frac{1}{\delta}$) decreases. For a fixed permeability of contact lens, this results in a decrease in the resistance offered by the frictional forces (that arise due to viscous-viscous interaction between the fluid layer and the porous layer) to the thinning of the pre-lens film. Hence, there is an increase in the thinning rate and advancement in finite-time rupture. This clearly explains the monotonic decreasing behaviour of rupture time as a function of porosity δ.

An increase in the stress-jump parameter χ increases the relative jump in the shear stresses at the interface. This causes reduction in the frictional forces which oppose the thinning of the pre-lens tear film. The rate of thinning of the film is increased and the life-span of the pre-lens tear film is advanced.

As the thickness of the contact lens increases, more and more of pre-lens tear film flows into the contact lens resulting in decrease in frictional forces that offer resistance to film thinning. Hence, the rate of thinning of pre-lens tear film is more on a thicker contact lens than on a film over a thinner contact lens. This increases the life span of tear film on a thinner contact lens.

Permeability describes the conductivity of a porous medium with respect to the flow of pre-lens tear film. It describes how easily a pre-lens tear film is able to move through the porous contact lens. Therefore, an increase in permeability of the contact lens decreases the amount of frictional forces that offer resistance to thinning. Hence, a pre-lens tear film over a contact lens with higher permeability has faster rate of thinning and this advances the rupture time as compared to that over a contact lens with lower permeability. This can also be inferred from the constant terms in the model, Eqs. (59)–(62). With an increase in Da, the contribution from the constant terms in both the models increases and it dominates the leading term of $O(h^3)$ resulting in an increase in the rate of thinning of pre-lens tear film over a contact lens with higher permeability. This advances the rupture time for a film over a contact lens with higher permeability.

Fig. 7 presents the results of the one-sided models derived for the shear-free case (Eq. (65)) and for the tangentially immobile case (Eq. (66)) along with the two-sided models (Eqs. (59) and (60) for the shear-free case and Eqs. (61) and (62) for the tangentially immobile case). The results are given for $Da = 10^{-8}$, $\delta = 0.1$, $\chi = 0.25$, and $H = 100$, when gravity is excluded (Fig. 7(a)) and when gravity is active (Fig. 7(b)). The dimensionless parameter l_{os} is calculated from $l_{os} = \frac{\sqrt{Da}(E_+ - E_-)}{B_+E_- + B_-E_+}$ using the above values of the parameters. The numerical results confirm the theoretically predicted results (presented in Table II) based on Bertozzi *et al.*[59] theory. For such small values of permeability and

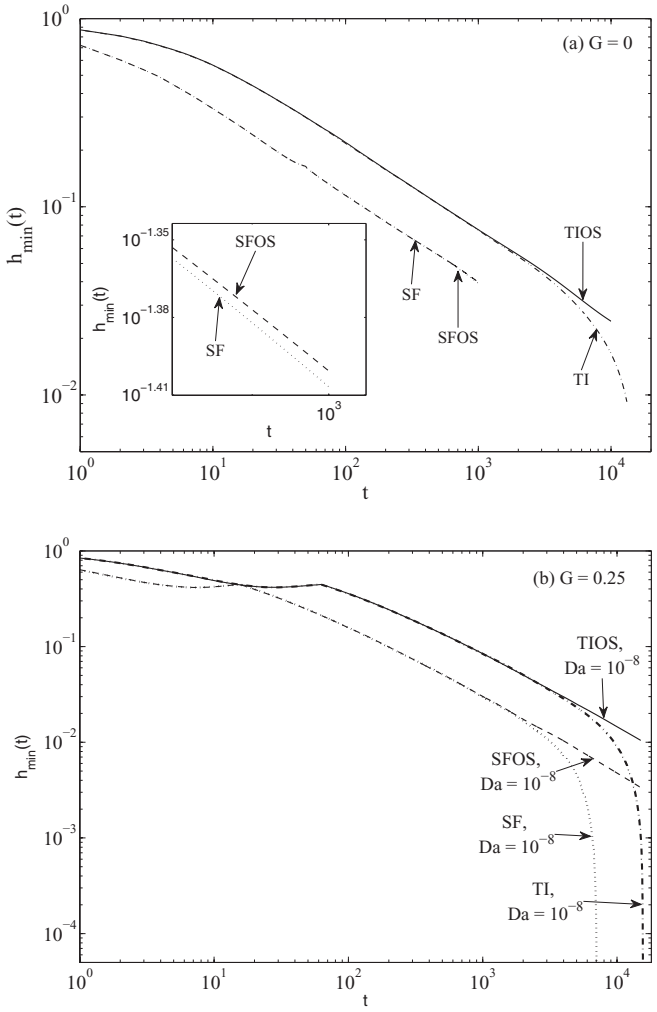

FIG. 7. Comparison of h_{min} values predicted by TIOS, TI, SFOS, and SF models when $H = 100$, $\delta = 0.1$, $\chi = 0.25$, $Da = 10^{-8}$. (a) $G = 0$. (b) $G = 0.25$.

porosity, the one-sided model results almost coincide with the two-sided model results for sufficiently long time in the both the cases ; however, beyond the dimensionless time of 10^3, the two-sided TI results show an increase in thinning of the pre-lens tear film leading to rupture (dashed-dotted curve; Fig. 7(a) for $G = 0$). The inset in Fig. 7(a) shows the corresponding comparison for the shear-free case (for $G = 0$) and for the time scales considered here. When gravity is included (Fig. 7(b)), the trend is the same as above for the TI models; however, for the shear-free case two-sided model, rate of thinning of the film increases beyond a certain dimensionless time and finite-time rupture occurs. The dynamics predicted by TI model is slower than that of SF model.

The long-time scenarios are presented in Fig. 8 for Le Bars-Worster (with slip parameter β) model[39] and Beavers-Joseph model[38] (with slip parameter $\frac{1}{\alpha}$) considered by Nong and Anderson[37] along with the results of the present model, when gravity effects are included.

The life-span of a pre-lens tear film predicted by the present model is longer than that predicted by the models of Nong and Anderson[37] (see the inset in Fig. 8). The thinning rate of the film predicted by Nong and Anderson[37] models are more than that of the present model. The presence of the porous contact lens is accounted for by taking into account the effects of permeability of the lens in their model. Their models employ a slip parameter ($1/\alpha$ in BJ model and β in LBW model) that accounts for the structure of the porous medium at the interface. An increase in the slip parameter ($1/\alpha$ or β) in their models corresponds to a decrease in velocity gradient and hence a decrease in the friction

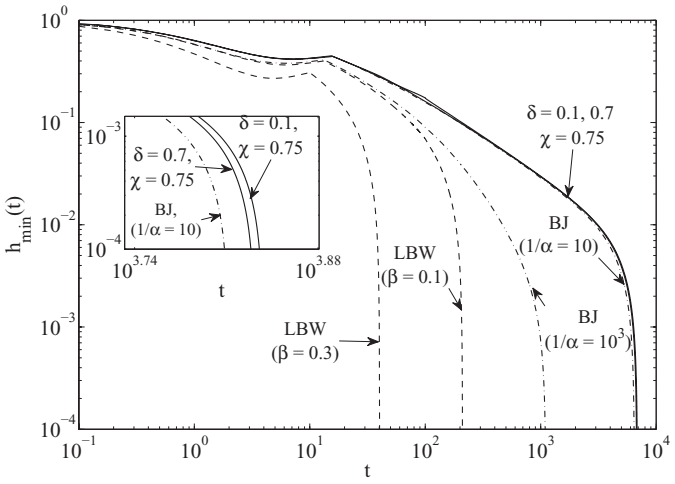

FIG. 8. Comparison of present model results (SF−solid curves; $\delta = 0.1$, $\chi = 0.75$; $\delta = 0.7$, $\chi = 0.75$) with Le Bars-Worster's slip (β) model (dashed curves) and Beavers-Joseph slip (α) model (dashed-dotted curves) results considered by Nong and Anderson,[37] when $H = 100$, $Da = 10^{-8}$, $G = 0.25$.

of the tear film with the bottom contact lens. The role of frictional forces is to offer resistance to thinning of the film. However, due to decrease in the frictional forces, the amount of frictional forces is not sufficient to offer resistance to thinning rate of the film. As a result, rate of thinning increases and finite-time rupture occurs at an earlier time in their models.

Also, the governing equations, under the lubrication approximation in the fluid and porous layers are

$$-p_x + u_{yy} + G\sin\theta = 0,$$

$$-Da\, p_x^b + Da\, G\sin\theta - u^b = 0$$

in Nong and Anderson's model,[37] while they are

$$-p_x + u_{yy} + G\sin\theta = 0,$$

$$-Da\, p_x^b + \frac{Da}{\delta}u_{yy}^b + Da\, G\sin\theta - u^b = 0$$

in the present study, respectively. For a given permeability of the contact lens, the contribution from $\frac{Da}{\delta}u_{yy}^b$ and u_{yy} to viscous-viscous interaction increases for a fixed δ (porosity parameter) and hence frictional forces that offer resistance to film thinning on a contact lens of thickness H increase in the present model as compared to the amount of frictional forces available in Nong and Anderson's[37] model. This reduces the rate of thinning of the film in the present model as compared to that in the models by Nong and Anderson[37] at earlier times. Also, there is a slow decrease of the thinning of the film and this delays the rupture time of the film in the present model as compared to that observed in Nong and Anderson[37] models. The inset in Fig. 8 shows the influence of porosity and stress-jump parameter.

V. CONCLUSION

The paper revisits a problem investigated by Nong and Anderson[37] by deriving a simple model for understanding the dynamics and rupture of a pre-lens tear film on a porous contact lens. The dynamics of pre-lens film has been coupled to the flow through the lens. This is done by using a Darcy-Brinkman model which describes the flow in the contact lens. The coupling then occurs through various boundary conditions at the contact lens/pre-lens interface. The evolution equation

for pre-lens tear film thickness has been obtained for shear free as well as for tangentially immobile free surface. The pre-lens tear film has surface tension helping to drive the flow and this flow is also affected by gravitational and viscous forces. The model equation for the evolution of film thickness in the present study are higher order models that describe the transport of momentum in the porous layer. This accounts for effective viscosity of the fluid in the porous layer (contact lens) and allows for viscous-viscous interaction at the interface of contact lens and pre-lens tear film. This gives rise to some terms in the evolution equation that become dominant as time progresses and they promote tear film thinning and eventually this leads to rupture of pre-lens tear film in finite time.

The nonlinear evolution is governed by two new parameters, namely, porosity δ and stress-jump parameter χ, in addition to permeability parameter (Da) and contact lens thickness H. The numerical results provide quantitative information on the effects of the parameters characterizing the contact lens. These indicate some differences in the results between the present model and the Darcy-based Nong and Anderson's[37] model. The differences are also observed in the long-time rupture behaviour as out lined in the context of the one-sided model. It is to be remarked that the differences that are most significant appear on time scales that are much longer than what would typically be of interest to the medical community that considers a typical blink time scale (<10 s) and for current contact lens designs.

Due to the nonavailability of the experimental work that can be directly applied to the present scenario, it has not been possible to compare the theoretical predictions of the present study with experimental data. However, some qualitative comparison of the present results can be observed from the experimental predictions by Nichols *et al.*[34] (not exactly relevant to the present study) on the rate of thinning of the pre-lens tear film, using interferometry as an *in vivo* measure of tear film thinning between blinks for hydrogel lens wearers. Their results show that the average thinning rate of the pre-lens tear film (PLTF) is more than that of the pre-corneal tear film (PCTF) and that as a consequence of this, the tear film thinning (time to reach zero thickness) is shorter for the pre-lens tear film than for pre-corneal tear film. This trend is captured by the present mathematical model where the results for $Da = 0$, $H = 0$ correspond to PCTF and that for non zero values of the parameters correspond to PLTF. The results of the present investigation lend themselves to verification by experiment.

The results of the present model reveal that the rupture time of the pre-lens tear film is advanced as the permeability of the lens is increased. This is due to the viscous-viscous interaction between the fluid and the porous layers that causes frictional forces which offer resistance to thinning of the film. This results in an increase in the rate of thinning at a higher permeability and rupture is advanced. The life span of a tear film on a thinner contact lens is longer for any permeability or porosity of the contact lens. The influence of porosity is to increase the rate of thinning of the tear film, resulting in advancement of rupture time for the film. The trend exhibited by the stress-jump parameter is analogous to that of the permeability/porosity of the lens. However, there is a delay in the rupture time predicted by the present model as compared to Nong and Anderson's[37] model using a contact lens with same thickness. This delay arises due to a combination of the influences of the viscous-viscous interaction, the permeability, the porosity, and the stress-jump parameters as explained in the discussion on the results presented in Tables III and IV. For realistic values of permeability and porosity of the contact lens, the effects are shown to be small and this may be due to the fact that important factors such as evaporation of the tear film and dynamics of post-lens film have not been incorporated in the model.

The central result in the present study is that using the higher order Darcy-Brinkman model to describe the dynamics in the contact lens, the pre-lens tear film over it has finite-time break up and this has profound implications for tear films over contact lens. Further, the results explain and demonstrate the important characteristics of the contact lens that cause the pre-lens tear film to rupture in the case of contact lens wearers. The model is developed to have a better understanding of the behaviour of pre-lens tear film over a porous contact lens. It is expected that the model might provide some information on the cause of dry-eye syndrome for wearers of contact lens.

It is of interest to develop more realistic models of pre-lens tear film that accounts for the post-lens film dynamics, evaporation, presence of lipid layer, motion of the ends of domain that describes blinking and the dynamics of the contact lens and this forms a part of future work.

It is hoped that such realistic models might provide the significant influence of the characteristics of the contact lens on the thinning rate and rupture of the pre-lens aqueous layer for time scales that would typically be of interest for blink cycles.

ACKNOWLEDGMENTS

The authors sincerely thank the referees for their very valuable comments and suggestions. These have helped in improving the content and quality of the paper. The authors also wish to thank the Editor, Professor G. Leal, for his useful remarks and suggestions.

APPENDIX: EVOLUTION EQUATION FOR THE TANGENTIALLY IMMOBILE CASE

The equation describing the evolution of pre-lens tear film thickness for the present study with tangentially immobile condition at the free surface is obtained as follows. The solutions of Eqs. (37)–(42) using the boundary conditions (43), (44), and (46)–(52) are given by

$$u = \frac{\mathrm{M}}{2}(y^2 - h^2) + \mathrm{A}_1(y - h), \tag{A1}$$

$$v = \mathrm{M}hh_x y + \mathrm{A}_1 h_x y - \mathrm{A}_{1x}\left(\frac{y^2}{2} - yh\right) - \mathrm{M}_x\left(\frac{y^3}{6} - \frac{y^2 h}{2}\right) + \mathrm{A}_3, \tag{A2}$$

$$u^b = \mathrm{C}_1 e^{\sqrt{\frac{\delta}{Da}}y} + \mathrm{C}_2 e^{-\sqrt{\frac{\delta}{Da}}y} - Da\mathrm{M}, \tag{A3}$$

$$v^b = -\sqrt{\frac{Da}{\delta}}\mathrm{C}_{1x} e^{\sqrt{\frac{\delta}{Da}}y} + \sqrt{\frac{Da}{\delta}}\mathrm{C}_{2x} e^{-\sqrt{\frac{\delta}{Da}}y} + Da\mathrm{M}_x y + \mathrm{B}_3, \tag{A4}$$

$$p = -\epsilon\, G\cos\theta(y - h) - h_{xx}, \tag{A5}$$

where

$$\begin{aligned}
\mathrm{A}_1 &= -\frac{1}{h}[\mathrm{C}_1 + \mathrm{C}_2 - Da\mathrm{M} + \frac{1}{2}\mathrm{M}h^2],\\
\mathrm{A}_3 &= \mathrm{C}_{1x}\sqrt{\frac{Da}{\delta}}(\mathrm{E}_- - 1) + \mathrm{C}_{2x}\sqrt{\frac{Da}{\delta}}(1 - \mathrm{E}_+) + Da\mathrm{M}_x H,\\
\mathrm{B}_3 &= \mathrm{C}_{1x}\sqrt{\frac{Da}{\delta}}\mathrm{E}_- - \mathrm{C}_{2x}\sqrt{\frac{Da}{\delta}}\mathrm{E}_+ + Da\mathrm{M}_x H,\\
\mathrm{C}_1 &= \frac{\mathrm{QE}_+ + Da\mathrm{M}(h\mathrm{B}_+ - \sqrt{Da})}{h\Delta + \sqrt{Da}(\mathrm{E}_+ - \mathrm{E}_-)}, \mathrm{C}_2 = \frac{-\mathrm{QE}_- + Da\mathrm{M}(h\mathrm{B}_- + \sqrt{Da})}{h\Delta + \sqrt{Da}(\mathrm{E}_+ - \mathrm{E}_-)},\\
Q &= -\mathrm{M}\sqrt{Da}\frac{h^2}{2} + Da^{\frac{3}{2}}\mathrm{M} - \chi\, Da\mathrm{M}h,\ \Delta = \mathrm{B}_+\mathrm{E}_- + \mathrm{B}_-\mathrm{E}_+,\\
\mathrm{B}_+ &= \frac{1}{\sqrt{\delta}} + \chi, \mathrm{B}_- = \frac{1}{\sqrt{\delta}} - \chi, \mathrm{E}_+ = e^{\sqrt{\frac{\delta}{Da}}H}, \mathrm{E}_- = e^{-\sqrt{\frac{\delta}{Da}}H},
\end{aligned} \tag{A6}$$

$$\mathrm{M}_{TI} = \epsilon G\cos\theta - \frac{1}{Ca}h_{xxx} - G\sin\theta. \tag{A7}$$

Substitution of Eqs. (A1)–(A7) in the kinematic boundary condition (43) yields the evolution equation for the TI case (Eqs. (61) and (62)).

[1] F. J. Holly, "Formation and rupture of the tear film," Exp. Eye Res. **15**, 515 (1973).
[2] R. E. Berger and S. Corrsin, "A surface tension gradient mechanism for driving the pre-corneal tear film after a blink," J. Biomech. **7**, 225 (1974).
[3] M. S. Norn, "Semiquantitative interference study of fatty layer of precorneal film," Acta Ophthalmol. **57**, 766 (1979).
[4] C. Franck, "Fatty layer of the precorneal film in the "office eye syndrome"," Acta Ophthalmol. **69**, 737 (1991).
[5] P. E. King-Smith, B. A. Fink, J. J. Nichols, K. K. Nichols, R. J. Braun, and G. B. McFadden, "The contribution of lipid layer movement to tear film thinning and breakup," Invest. Ophthalmol. Visual Sci. **50**, 2747 (2009).
[6] N. Ehlers, "The precorneal film: Biomicroscopical, histological and chemical investigations," Acta Ophthalmol. Suppl. **81**, 3 (1965).
[7] S. Mishima, "Some physiological aspects of the precorneal tear film," Arch. Ophthalmol. **73**, 233 (1965).
[8] E. Wilson, *Anatomy of Eye and Orbit*, 4th ed. (Blakiston, New York, 1954).
[9] A. Sharma, "Acid-base interactions in the cornea-tear film system: surface chemistry of corneal wetting, cleaning, lubrication, hydration and defense," J. Dispersion Sci. Technol. **19**, 1031 (1998).
[10] A. Sharma, R. Khanna, and G. Reiter, "A thin film analog of the corneal mucus layer of the tear film: an enigmatic long range non-classical DLVO interaction in the breakup of thin polymer films," Colloids Surf., B **14**, 223 (1999).
[11] Y. L. Zhang, O. K. Matar, and R. V. Craster, "Analysis of tear film rupture: Effect of non-Newtonian rheology," J. Colloid Interface Sci. **262**, 130 (2003).
[12] Y. L. Zhang, R. V. Craster, and O. K. Matar, "Surfactant driven flows overlying a hydrophobic epithelium: film rupture in the presence of slip," J. Colloid Interface Sci. **264**, 160 (2003).
[13] R. J. Braun and A. D. Fitt, "Modelling drainage of the precorneal tear film after a blink," Math. Med. Biol. **20**, 1 (2003).
[14] I. Fatt and B. Weissman, *Physiology of the Eye: An introduction to the Vegetative Functions*, 2nd ed. (Butterworth-Heinemann, Boston, 1992).
[15] A. J. Bron, J. M. Tiffany, S. M. Gouveia, N. Yokoi, and L. W. Voon, "Functional aspects of the tear film lipid layer," Exp. Eye Res. **78**, 347 (2004).
[16] J. P. McCulley and W. Shine, "A compositional based model for the tear film lipid layer," Trans. Am. Ophthalmol. Soc. **95**, 79 (1997).
[17] I. K. Gipson, "Distribution of mucins at the ocular surface," Exp. Eye Res. **78**, 379 (2004).
[18] I. Cher, "Another way to think of tears: Blood, sweat, and . . . Dacruon," Ocul. Surf. **5**, 251 (2007).
[19] M. Rolando and M. Zierhut, "The ocular surface and tear film and their dysfunction in dry eye disease," Surv. Ophthalmol. **45**(S2), S203 (2001).
[20] A. Sharma and E. Ruckenstein, "Mechanism of tear film rupture and formation of dry spots on cornea," J. Colloid Interface Sci. **106**, 12 (1985).
[21] H. Wong, I. Fatt, and C. J. Radke, "Deposition and thinning of the human tear film," J. Colloid Interface Sci. **184**, 44 (1996).
[22] K. N. Winter, D. M. Anderson, and R. J. Braun, "A model for wetting and evaporation of a post-blink precorneal tear film," Math. Med. Biol. **27**, 211 (2010).
[23] M. B. Jones, C. P. Please, D. L. S. McElwain, G. R. Fulford, A. P. Roberts, and M. J. Collins, "Dynamics of tear film deposition and draining," Math. Med. Biol. **22**, 265 (2005).
[24] A. Heryudono, R. J. Braun, T. A. Driscoll, L. P. Cook, K. L. Maki, and P. E. King-Smith, "Single-equation models for the tear film in a blink cycle: realistic lid motion," Math. Med. Biol. **24**, 347 (2007).
[25] R. J. Braun and P. E. King-Smith, "Model problems for the tear film in a blink cycle: single equation models," J. Fluid Mech. **586**, 465 (2007).
[26] K. L. Maki, R. J. Braun, T. A. Driscoll, and P. E. King-Smith, "An overset grid method for the study of reflex tearing," Math. Med. Biol. **25**, 187 (2008).
[27] K. L. Maki, R. J. Braun, W. D. Henshaw, and P. E. King-Smith, "Tear film dynamics on an eye-shaped domain I: pressure boundary conditions," Math. Med. Biol. **27**, 227 (2010).
[28] K. L. Maki, R. J. Braun, W. D. Henshaw, and P. E. King-Smith, "Tear film dynamics on an eye-shaped domain. Part 2. Flux boundary conditions," J. Fluid Mech. **647**, 361 (2010).
[29] R. J. Braun, R. Usha, G. B. McFadden, T. A. Driscoll, L. P. Cook, and P. E. King-Smith, "Thin film dynamics on a prolate spheroid with application to the cornea," J. Eng. Math. **73**, 121 (2012).
[30] R. J. Braun, "Dynamics of the tear film," Annu. Rev. Fluid Mech. **44**, 267 (2012).
[31] L. Li and R. J. Braun, "A model for the human tear film with heating from within the eye," Phys. Fluids **24**, 062103 (2012).
[32] M. B. Jones, D. L. S. McElwain, G. R. Fulford, M. J. Collins, and A. P. Roberts, "The effect of the lipid layer on tear film behavior," Bull. Math. Biol. **68**, 1355 (2006).
[33] J. J. Nichols and P. E. King-Smith, "Thickness of the pre- and post-contact lens tear film measured *in vivo* by interferometry," Invest. Ophthalmol. Visual Sci. **44**, 68 (2003).
[34] J. J. Nichols, G. L. Mitchell, and P. E. King-Smith, "Thinning rate of the precorneal and prelens tear films," Invest. Ophthalmol. Visual Sci. **46**, 2353 (2005).
[35] F. Fornasiero, J. M. Prausnitz, and C. J. Radke, "Post-lens tear-film depletion due to evaporative dehydration of a soft contact lens," J. Membr. Sci. **275**, 229 (2006).
[36] L. C. Thai, A. Tomlinson, and M. G. Doane, "Effect of contact lens material on tear physiology," Optom. Vision Sci. **81**, 194 (2004).
[37] K. Nong and D. M. Anderson, "Thin film evolution over a thin porous layer: Modeling a tear film on a contact lens," SIAM. J. Appl. Math. **70**, 2771–2795 (2010).
[38] G. S. Beavers and D. D. Joseph, "Boundary conditions at a naturally permeable wall," J. Fluid Mech. **30**, 197 (1967).
[39] M. Le Bars and M. G. Worster, "Interfacial conditions between a pure fluid and a porous medium: Implications for binary alloy solidification," J. Fluid Mech. **550**, 149 (2006).

[40] B. Goyeau, D. Lhuillier, D. Gobin, and M. G. Velarde, "Momentum transport at a fluid-porous interface," Int. J. Heat Mass Transfer **46**, 4071 (2003).
[41] P. Bousquet-Melou, B. Goyeau, M. Quintard, F. Fichot, and D. Gobin, "Average momentum equation for interdendritic flow in a solidifying columnar mushy zone," Int. J. Heat Mass Transfer **45**, 3651 (2002).
[42] J. A. Ochoa-Tapia and S. Whitaker, "Momentum transfer at the boundary between a porous medium and a homogeneous fluid-I. Theoretical development," Int. J. Heat Mass Transfer **38**, 2635 (1995).
[43] J. A. Ochoa-Tapia and S. Whitaker, "Momentum transfer at the boundary between a porous medium and a homogeneous fluid-II. Comparison with experiment," Int. J. Heat Mass Transfer **38**, 2647 (1995).
[44] U. Thiele, B. Goyeau, and M. G. Velarde, "Stability analysis of thin film flow along a heated porous wall," Phys. Fluids **21**, 014103 (2009).
[45] S. Whitaker, "Flow in porous media I: A theoretical derivation of Darcy's law," Transp. Porous Media **1**, 3 (1986).
[46] D. A. Nield and A. Bejan, *Convection in Porous Media* (Springer-Verlag, New York, 1992).
[47] S. D. R. Wilson, "The drag-out problem in film coating theory," J. Eng. Math. **16**, 209 (1982).
[48] D. Miller, "Measurement of the surface tension of tears," Arch. Opthalmol. **82**, 368 (1969).
[49] P. E. Raad and A. S. Sabau, "Dynamics of a gas permeable contact lens during blinking," ASME Trans. J. Appl. Mech. **63**, 411 (1996).
[50] C. Maldonado-Codina and N. Efron, "Impact of manufacturing technology and material composition on the clinical performance of hydrogel lenses," Optom. Vision Sci. **81**, 442 (2004).
[51] M. V. Monticelli, A. Chauhan, and C. J. Radke, "The effect of water hydraulic permeability on the settling of a soft contact lens on the eye," Curr. Eye Res. **30**, 329 (2005).
[52] T. T. Hayashi, "Mechanics of contact lens motion," Ph.D dissertation (University of California, Berkeley, 1977).
[53] D. K. Martin, J. Boulos, J. Gan K. Gavriel, and P. Harvey, "A unifying parameter to describe the clinical mechanics of hydrogel contact lenses," Optom. Vision Sci. **66**, 87 (1989).
[54] S. H. Davis and L. M. Hocking, "Spreading and imbibition of viscous liquid on a porous base," Phys. Fluids **11**, 48 (1999).
[55] S.H. Davis and L. M. Hocking, "Spreading and imbibition of viscous liquid on a porous base. II," Phys. Fluids **12**, 1646 (2000).
[56] H. P. Greenspan, "On the motion of a small viscous droplet that wets a surface," J. Fluid Mech. **84**, 125 (1978).
[57] L. M. Hocking, "Sliding and spreading of thin two-dimensional drops," Q. J. Mech. Appl. Math. **34**, 37 (1981).
[58] I. M. R. Sadiq and R. Usha, "Thin Newtonian film flow down a porous inclined plane: Stability analysis," Phys. Fluids **20**, 022105 (2008).
[59] A. L. Bertozzi, M. P. Brenner, T. F. Dupont, and L. P. Kadanoff, "Singularities and similarities in interface flows," in *Trends and Perspectives in Applied Mathematics*, Applied Mathematical Sciences, edited by L. Sirovich (Springer-Verlag, New York, 1994), Vol. 100, p. 155.
[60] A. L. Bertozzi, "Symmetric singularity formation in lubrication-type equations for interface motion," SIAM J. Appl. Math. **56**, 681 (1996).